

[Click here to view linked References](#)

1 ***Streptomyces tsukubaensis* as a new model for carbon**
2 **repression: transcriptomic response to tacrolimus repressing**
3 **carbon sources**

4 **María Ordóñez-Robles^{1,2}, Fernando Santos-Beneit^{2,3}, Silvia M. Albillos^{2,4}, Paloma Liras^{1,2}, Juan F.**
5 **Martín^{1,2}, and Antonio Rodríguez-García^{1,2}.**

6 1) Área de Microbiología, Facultad de Ciencias Biológicas y Ambientales, Universidad de León, 24071
7 León, Spain

8 2) Instituto de Biotecnología de León, INBIOTEC, Avda. Real no. 1, 24006 León, Spain

9 3) Current address: Centre for Bacterial Cell Biology, Institute for Cell and Molecular Biosciences,
10 Medical School, Newcastle University, Newcastle upon Tyne, UK

11 4) Current address: Departamento de Biotecnología y Ciencia de los Alimentos, Facultad de Ciencias,
12 Universidad de Burgos, 09001 Burgos, Spain

13 Corresponding authors: Antonio Rodríguez-García and María Ordóñez-Robles.

14 E-mail: antonio.rodriguez@inbiotec.com (Tlf: +34 987 21 03 08); mordr@unileon.es.

15 **Key words:** *Streptomyces tsukubaensis*, tacrolimus, FK506, carbon regulation, transcriptomics.

16 **Acknowledgements**

17 This work was supported by the European Union through an ERA-IB (PIM2010EEI-00677) international
18 cooperation project. M. Ordóñez-Robles received a FPU fellowship of the Ministerio de Educación y
19 Ciencia (Spain). We thank Dr. C. Prieto for sharing their prediction results of intrinsic terminators that
20 were included in the microarray probe design. We acknowledge the technical support of B. Martín, J.
21 Merino, A. Casenave and A. Mulero (INBIOTEC).

29 **ABSTRACT**

30 In this work, we identified glucose and glycerol as tacrolimus repressing carbon sources in the important
31 species *Streptomyces tsukubaensis*. A genome-wide analysis of the transcriptomic response to glucose
32 and glycerol additions was performed using microarray technology. The transcriptional time series
33 obtained allowed us to compare the transcriptomic profiling of *S. tsukubaensis* growing under tacrolimus
34 producing and non-producing conditions. The analysis revealed important and different metabolic
35 changes after the additions and a lack of transcriptional activation of the *fkb* cluster. In addition, we
36 detected important differences in the transcriptional response to glucose between *S. tsukubaensis* and the
37 model species *Streptomyces coelicolor*. A number of genes encoding key players of morphological and
38 biochemical differentiation were strongly and permanently downregulated by the carbon sources. Finally,
39 we identified several genes showing transcriptional profiles highly correlated to that of the tacrolimus
40 biosynthetic pathway regulator FkbN that might be potential candidates for the improvement of
41 tacrolimus production.

42

43

44

45

46

47

48

49

50

51

52

53

54

55

56

57

58

59 **INTRODUCTION**

1
2 60 Strains of the gram-positive, soil-dwelling bacterial genus *Streptomyces* stand out for their ability to
3
4 61 produce a wide range of secondary metabolites with biological activity. In fact, more than a half of the
5
6 62 antibiotics from microbial origin used in clinics are produced by this genus (Hopwood 2007).
7
8 63 *Streptomyces tsukubaensis* (Kino et al. 1987a; 1987b) is an important industrial species which produces
9
10 64 tacrolimus (or FK506), a 23-membered macrolide showing immunosuppressant activity that is widely
11
12 65 used in the prevention of graft rejection and in the treatment of skin diseases. Despite of its clinical
13
14 66 relevance and the generation of important benefits for the pharmaceutical market, low production levels
15
16 67 are achieved by industrial strains (Barreiro and Martínez-Castro 2014). Improvement of FK506
17
18 68 production has been obtained through culture media optimization and genetic engineering of the strains.
19
20 69 Nevertheless, the identification of transcriptional regulators that might be involved in the regulation of its
21
22 70 biosynthesis is of high interest to achieve further improvements.

23
24 71 The presence of carbon sources in the culture media that are rapidly assimilated blocks or reduces the
25
26 72 production of secondary metabolites and such regulation can take place at the enzymatic and/or at the
27
28 73 transcriptional level (reviewed in Ruiz et al. 2010). This phenomenon resembles carbon catabolite
29
30 74 repression (CCR; Magasanik 1961), which prevents the use of alternative carbon sources in the presence
31
32 75 of “preferred” ones (usually glucose). As it can be deduced, CCR is an important barrier for the
33
34 76 production of bioactive compounds, since preferred carbon sources that would allow a faster growth
35
36 77 hamper secondary metabolite production. Thus, avoiding or reducing CCR is an important strategy to
37
38 78 improve secondary metabolite production and, for this purpose, understanding its regulation is highly
39
40 79 necessary. Despite of its importance, the molecular mechanisms that govern CCR in the genus
41
42 80 *Streptomyces* are still not completely elucidated. A key player in *Streptomyces* CCR is the glycolytic
43
44 81 enzyme glucose kinase (Glk), which is proposed to interact with transcriptional regulators in order to
45
46 82 exert its regulatory role (Angell et al. 1992). Nevertheless, Glk is not the sole responsible for
47
48 83 *Streptomyces* CCR; other players such as SCO2127 or Rok7b7 are involved (Angell et al. 1992; Gubbens
49
50 84 et al. 2012).

51
52 85 Since “omic” approaches represent a useful tool to study regulatory networks, the aim of this work was i)
53
54 86 to identify FK506 repressing carbon sources in *S. tsukubaensis* and ii) to study their effect on the whole
55
56 87 transcriptome and establish a comparison between the transcriptional behaviour of this strain under
57
58 88 FK506 producing and non-producing conditions. By this mean we aimed to identify key regulators that
59
60 89 might be involved in FK506 production and/or in the mechanisms governing CCR. Transcriptomics have
61
62 90 been applied recently to the study of *S. coelicolor* CCR in a one-point experimental design corresponding
63
64 91 to the exponential growth phase (Romero-Rodríguez et al. 2016a; 2016b). In this work, we performed a
65
66 92 10-point transcriptional time series comprising all the growth phases. Such design enables the comparison
67
68 93 not only between producing and non-producing conditions but also between primary and secondary
69
70 94 metabolism. Here we describe the main transcriptional changes observed after glucose and glycerol
71
72 95 additions and present new candidates for the improvement of FK506 production and the study of key
73
74 96 *Streptomyces* biology aspects.

97 MATERIALS AND METHODS

98 Bacterial strains and growth conditions

99 *Streptomyces tsukubaensis* (Kino et al. 1987a) was grown at 28 °C on ISP4 (Difco™, BD, NJ, USA)
100 medium for spore preparation. For FK506 production studies, 10⁹ spores of *S. tsukubaensis* were
101 inoculated into 0.5-l flasks containing 100 ml of MGm-2.5 media (Martínez-Castro et al. 2013) and
102 incubated at 28 °C and 220 rpm. Carbon sources added to the cultures, such as glycerol, mannitol (both
103 form Prolabo-VWR, Radnor, PA, USA), D-fructose (Merck, Darmstadt, Germany), maltose monohydrate
104 (SAFC-Sigma, Madison, WI, USA), xylose, D-glucose monohydrate (both from Sigma-Aldrich, St. Luis,
105 MI, USA), sucrose (NormaPur--VWR, Radnor, PA, USA) and lactose monohydrate (Rectapur--VWR,
106 Radnor, PA, USA), were dissolved in hot Milli-Q water (65 °C) and sterilized at 120 °C for 15 minutes.
107 The final concentrations in the culture media are indicated in the corresponding section.

108 The FK506-sensitive strain *Saccharomyces cerevisiae* TB23 (Breuder et al. 1994) was cultured in YPD
109 media (Lodder, 1970) at 28 °C and 250 rpm.

110 Growth measurement, FK506 and phosphate determination

111 For growth measurement and phosphate determination, 2-ml culture samples were harvested and
112 centrifuged. The supernatant was collected for inorganic phosphate determination using the malachite
113 green assay (Lanzetta et al. 1979). The pellet was washed twice with Milli-Q® water and dried at 80 °C
114 for 48 hours for growth determination.

115 For FK506 extraction, 1-ml culture samples were mixed with an equal volume of methanol (HPLC grade)
116 in 10-ml tubes. The mixtures were shaken in a horizontal position for one hour at 140 rpm and
117 centrifuged. The supernatants were collected and FK506 concentration was measured with an Agilent
118 HPLC equipped with a Zorbax SB C18 column (4.6x150 mm, 3.5 µm) following the indications from
119 Salehi-Najafabadi and coworkers (2014). Standards of pure FK506 (Antibióticos de León SLU, Spain)
120 and ascomycin (Sigma-Aldrich, St. Luis, MI, USA) were used as controls.

121 During the screening for repressing carbon sources, antifungal activity in the extracts was detected by
122 bioassay against *S. cerevisiae* TB23 (Breuder et al. 1994) as indicated by Ordóñez-Robles and coworkers
123 (2016).

124 RNA extraction and purification, labelling and hybridization

125 All the procedures related to the extraction and purification of RNA, the synthesis of labeled cDNA and
126 the conditions used for microarray hybridization were performed as previously described (Ordóñez-
127 Robles et al. 2016). Samples for RNA extraction were taken at 70 h (immediately before the additions),
128 70.7 h, 72 h, 76 h, 80 h, 89 h, 92 h, 100 h, 124 h and 148 h.

129 Microarray design and data analysis

130 The custom microarrays used in this work were manufactured by Agilent Technologies (Santa Clara, CA,
131 USA) in the 8×15K format. The expression probes (45- to 60-mer) were designed using the online tool
132 eArray from Agilent. In addition, tiling probes covering the coding strand of the FK506 biosynthetic
133 cluster (*fkb*) were designed using the chipD program (Dufour et al. 2010).

134 The limma package v3.20 (Smyth 2004) was used for normalization of the signal intensities and also for
135 statistical analyses following the indications in Ordóñez-Robles and coworkers (2016). After
136 normalization we obtained a final M_g value (\log_2 transcription value), which is an approximate measure
137 of the abundance of the transcripts of a particular gene with respect to its genomic copies (Mehra et al.
138 2006; Sidders et al. 2007). To find differentially expressed genes limma calculated the M_c values, which
139 represent the \log_2 -fold change between two experimental conditions (i. e. differences between selected M_g
140 values). Limma also provided the adjusted p -values (named p_{FDR}) to control the false discovery rate
141 (Benjamini and Hochberg 1995). The maSigPro software (Conesa et al. 2006), from the Bioconductor 3.2
142 package, was used to find genes showing different transcription profiles between experimental conditions
143 during the five first time points of the series. To detect transcriptional profiles similar to that of the
144 transcriptional regulator coding gene *fkbN*, we analyzed Pearson correlation coefficients.

145 **Quantitative reverse transcription PCR (RT-qPCR)**

146 To validate the microarray results by RT-qPCR, we used the primer pairs listed in Table S1 and the
147 procedures indicated by Ordóñez-Robles and coworkers (2016). cDNA originated from the RNA samples
148 was used to measure transcript levels of *pfkA1*, *pfkA2*, *pfkA3*, *amtB*, *hrdA*, *gltD*, *fkbN*, *glpX*, *crp* and *phoP*.
149 For normalizing assays, *metF* and *gyrB* genes were chosen since their M_g levels were among the most
150 constant throughout the time series. A high correlation ($R^2 = 0.78$) between microarray-derived and RT-
151 qPCR transcriptional ratios validated the results (see Fig S1).

152 **RESULTS**

153 **Experimental setup**

154 *Identification of FK506-repressing carbon sources*

155 The first goal of this work was to identify carbon sources that repress FK506 production in
156 *S. tsukubaensis*. For this purpose, *S. tsukubaensis* was grown in defined MGm-2.5 medium (Martínez-
157 Castro et al. 2013), a production medium containing starch as main carbon source, glutamate as carbon
158 and nitrogen source and limited in phosphate. This medium supports a good and dispersed growth and
159 high yields of FK506 production. FK506 biosynthesis is triggered after phosphate depletion, which
160 occurs between 80 h-89 h. We selected a set of 8 carbon sources (glucose, fructose, xylose, glycerol,
161 mannitol, maltose, lactose and sucrose) for the study, including the most common repressing sources
162 glucose and glycerol (for a review on *Streptomyces* carbon repression see Ruiz et al. 2010). The presence
163 of the carbon sources in the growth media from the beginning of the fermentation was rejected since
164 growth rate variations might difficult the interpretation of the results (Lounes et al. 1996). The accurate
165 study of the response to carbon source additions requires all cultures to be at the same physiological state

166 before the addition. Thus, the carbon sources were added during the first growth phase and before the
167 depletion of phosphate (i.e. 70 h).

168 The repressing effect of a carbon source depends on its concentration; for example, glucose at final
169 concentrations between 1-1.75 % has a positive effect on FK506 production in several *S. tsukubaensis*
170 ZJU01 strains (Chen et al. 2012). Thus, a high final concentration (2.8 % w/v) for all the carbon sources
171 tested was selected for this exploratory experiment. Culture samples for dry weight (from 64 h to 161 h)
172 and FK506 determination (from 92 h to 161 h) were taken. The presence of FK506 in the culture
173 supernatants was tested by agar diffusion bioassays against *S. cerevisiae* TB23. The addition of these
174 carbon sources did not affect growth (data not shown) and only glucose and glycerol inhibited FK506
175 production (see Table S2). Thus, glucose and glycerol were selected to perform the transcriptomic
176 analysis.

177 *Time-series cultures for transcriptomic analyses*

178 For the transcriptomic analysis, *S. tsukubaensis* was cultured under the same conditions indicated above,
179 adding glucose or glycerol as repressing carbon sources at 70 h. A control condition was included
180 consisting on the addition of maltose, since this disaccharide does not repress FK506 production and is a
181 natural product of starch metabolism. For each experimental condition five replicates were cultured. The
182 final concentrations of glucose and glycerol were established at the same molarity (0.22 M; 2 % w/v and
183 4 % w/v for glucose and glycerol, respectively). The final concentration of maltose was established at
184 0.11 M (3 % w/v) in order to equalize the number of glucose molecules available after maltose
185 incorporation. Samples for dry weight, phosphate concentration and FK506 determination were taken
186 between 65 h and 235 h from the five replicates of each culture condition. Samples for RNA extraction
187 were taken at 70 h (immediately before additions), and then from 70.7 h to 148 h (see Materials and
188 Methods).

189 According to their growth curves and the pattern of phosphate depletion, two cultures from each
190 experimental condition were selected for RNA extraction in order to ensure the highest physiological
191 homogeneity. The growth, phosphate depletion and FK506 production patterns of the six cultures (two
192 from each experimental condition) are depicted in Fig 1. In the control condition, FK506 production
193 started after phosphate depletion (89 h), as expected, since this is the limiting nutrient in this medium.
194 FK506 reached its maximum specific production values at 148 h (see Fig 1b). Glucose addition blocked
195 FK506 production along the whole time course of the cultures. The addition of glycerol repressed
196 production at least during the first 161 h of culture, although FK506 was detected at the last sample time
197 (235 h).

198 **Immediate response to the repressing carbon sources**

199 In order to identify genes that respond quickly to the carbon source additions, a comparison of the M_g
200 transcription values at 70 h ($t_{70\text{ h}}$) (i.e., immediately before the addition) with the $M_g t_{70.7\text{ h}}$ values (i. e., 40
201 minutes after the addition) was performed using the limma package. This approach yielded a total of 1176
202 genes as differentially transcribed after the additions (203 of them with 2-fold or greater changes). In

203 addition, a regression approach for the first five time-point values ($t_{70.7\text{ h}} - t_{80\text{ h}}$) of each experimental
204 condition was applied using maSigPro to identify genes affected by the additions that might not be
205 detected with the first approach. From this analysis, a total of 1315 genes showed statistically significant
206 differences (255 of them with $R^2 \geq 0.9$). Finally, we focused our functional analysis on a set of 361 genes
207 showing the strongest differences in any of both approaches (203 and 255 for limma and maSigPro,
208 respectively; see Fig S2). These genes are listed in Table S3. The fact that only 63 genes out of 361
209 showed significant transcriptional variations 40 min after maltose addition supported the choice of this
210 disaccharide as the control addition.

211 *Effects on carbon source transport*

212 First, we focused our attention on the genes encoding the putative transporters for maltose, glucose and
213 glycerol even if most of them were not filtered in the statistical analysis. The maltose ABC transporter
214 genes *malEFG* were downregulated after the three additions, especially after maltose addition (Fig S3.1)
215 and, although not included with the approaches used, the changes were statistically significant $t_{70.7\text{h}}$ and
216 $t_{72\text{h}}$ for glycerol and maltose conditions, respectively. Transcription of the operon for glycerol transport
217 and metabolism increased after glycerol addition and was transiently downregulated by glucose (Fig
218 S3.2), which was in accordance with the results reported in *S. coelicolor* (Smith and Chater 1988). On the
219 contrary, transcription of the unique glucose permease coding gene, *glcP*, was low throughout the culture
220 and not induced after glucose addition (Fig S3.3), which contrasts with its behavior in *S. coelicolor* (van
221 Wezel et al. 2005). In *S. tsukubaensis*, as well as in *Streptomyces clavuligerus* and
222 *Streptomyces avermitilis*, only one *glcP* gene is found. This gene is orthologue to *S. coelicolor glcP2*,
223 which inactivation does not affect glucose transport in this species (van Wezel et al. 2005). In the
224 upstream region of *glcP* we did not detect bacterial sigma 70 promoters using the online tool BPROM
225 (Solovyev and Salamov 2011). This situation resembles that of *S. clavuligerus*, where the weakly
226 expression of *glcP* accounts for the lack of growth on glucose as the sole carbon source (Pérez-Redondo
227 et al. 2010). Thus, it is possible that transcription of *S. tsukubaensis glcP* depends on a non-constitutive
228 sigma factor and that under our culture conditions an alternative transporter is responsible for the
229 incorporation of glucose. Indeed, two different glucose transporters have been biochemically reported in
230 *Streptomyces lividans* (Hurtubise et al. 1995).

231 We detected a high number of genes encoding transport-related functions that were affected by the
232 additions (amino acid and oligopeptide transporters related with differentiation are discussed in the
233 corresponding sections). As it might be expected from the concept of CCR, both additions reduced the
234 mRNA levels of genes encoding transporters for alternative carbon sources. This response was significant
235 at $t_{70.7\text{h}}$ and $t_{72\text{h}}$ for glucose and glycerol additions, respectively (Fig S3.4). Among the affected genes we
236 detected STSU_23336 (homolog to *nagE2*, encoding the predicted N-acetylglucosamine specific IIC
237 component of the PTS system), *dasA* (encoding the chitobiose transporter; Saito et al. 2007) and *msiK*
238 (encoding an ATP-binding protein which is involved in the transport of several carbon sources; van
239 Wezel et al. 1997). Transcription of the xylose transport operon *xyIFGH* was also downregulated after the
240 additions (Fig S3.4), which is in contrast to that reported in the model strain (Romero-Rodríguez et al.
241 2016a). This evidences important metabolic differences between *Streptomyces* strains.

242 Interestingly, glucose addition exerted a positive effect on several genes related to xylose metabolism.
243 Transcription of two xylose isomerase coding genes (*xylA* and STSU_23777) and other xylose isomerase
244 domain containing genes (i.e. STSU_04768, which was also transiently upregulated after maltose
245 addition) were upregulated by glucose (Fig S3.5). In *S. coelicolor* xylose transport and xylose metabolism
246 genes are regulated independently (Swiatek et al. 2013) and glucose stimulates 10-fold the transcription
247 of the xylose transporter genes *xylFGH* (SCO6009-SCO6011; Romero-Rodríguez et al. 2016a). In *S.*
248 *tsukubaensis* we observed the opposite behaviour for xylose transporter genes, which were downregulated
249 after glucose addition (see Fig S3.4). This phenomenon might be due to an anticipative regulatory
250 mechanism in which the presence of a common metabolite from glucose and xylose utilization pathways
251 stimulates transcription of genes involved in xylose catabolism. Anticipation to environmental changes is
252 a feature observed in both eukaryots and prokaryots and favoured through the evolution (Mitchell et al.
253 2009).

254 Closely located to STSU_04768, we found an ABC transporter operon (STSU_04793-STSU_04803)
255 which was transcriptionally activated after glucose and maltose additions. This operon might encode a
256 ribose transporter and is likely to be regulated by the ROK family transcriptional regulator STSU_04808,
257 which is encoded upstream and showed a similar transcriptional pattern after glucose and maltose
258 additions (Fig S3.6).

259 Interestingly, transcription of the xylose isomerase coding gene STSU_23777 showed the same
260 transcriptional profile than STSU_23771 (encoding a LysR type regulator) and STSU_23786 (encoding a
261 MarR family regulator; Fig S3.7). The transcription of STSU_23786 showed one of the highest increases
262 detected in mRNA levels after the glucose addition (i.e. 4.7 log₂-fold change).

263 *Effects on central carbon pathways*

264 Glucose addition upregulated the transcription of several genes involved in the glycolytic pathway such
265 as *pfkA3* (coding the 6-phosphofructokinase 3), *tpiA* (coding a triose-phosphate isomerase; this gene was
266 not filtered and, thus, is not included in Table S3) and *pgk* (coding a phosphoglycerate kinase). It also
267 increased the transcription of the gluconate kinase coding gene *idnK* (see Fig 2 and Fig S3.8). This is in
268 agreement to that reported for the orthologue SCO1679 in *S. coelicolor*, although we did not detect
269 upregulation of genes encoding gluconate dehydrogenases (Romero-Rodríguez et al. 2016a). In
270 agreement with these results, we observed a decrease in the mRNA levels of genes involved in the
271 gluconeogenic pathway (i.e. the rate controlling phosphoenolpyruvate carboxykinase encoded by *pck*, the
272 glyceraldehyde-3-phosphate dehydrogenase 2 coding gene *gap2* and the fructose-1,6-biphosphate aldolase
273 encoded by *glpX*; see Fig S3.9). Glucose upregulated transcription of genes involved in the formation of
274 pyruvate (pyruvate kinase 2 *pyk2*; this gene was not filtered and thus, is not included in Table S3) and
275 oxaloacetate (phosphoenolpyruvate carboxylase *ppc*; Fig S3.9) but downregulated some genes involved in
276 the tricarboxylic acid (TCA) cycle (i.e. malate oxidoreductase *mals4*, succinate dehydrogenases *sdhB* and
277 *sdhA* and citochrome b subunit *sdhC2*; Fig S3.10). These results are in contrast with those reported for *S.*
278 *coelicolor* by Romero-Rodríguez and coworkers (2016a), who suggested that TCA enzymes might be
279 regulated by metabolites rather than at the transcriptional level.

280 The effect of glycerol addition on carbon central pathways was narrower compared to that of glucose. The
281 responses detected were limited to the downregulation of *pgk* (encoding the bifunctional
282 phosphoglycerate kinase from glycolysis), and *bglA2* (encoding a sugar hydrolase similar to the 6-
283 phospho-beta-glucosidase that generates glucose and glucose-6-phosphate; see Fig S3.8 and S3.9.
284 Glycerol upregulated transcription of the TCA gene *fumC* (encoding a fumarase; Fig S3.10). In
285 *Escherichia coli*, FumC is produced only under low iron availability or when superoxide radicals
286 accumulate, whilst in *Bacillus subtilis* the expression is induced by fumarate and repressed by glucose
287 addition (Park and Gunsalus 1995; Ohné 1975).

288 Both additions exerted a negative effect on the transcription of genes involved in fatty acid degradation
289 and upregulated transcription of genes involved in the biosynthesis of phospholipids or encoding lipases.
290 Glucose and glycerol additions stimulated transcription of genes involved in fatty acid biosynthesis such
291 as *accB*, *accE* and *fabH* (Fig S3.11). *accB* and *accE* encode an acyl-CoA carboxylase which catalyzes the
292 formation of malonyl-CoA from acetyl-CoA. This enzyme has been reported to be directly involved in
293 the production of pigmented antibiotics in the model *S. coelicolor*, since mutants in *accB* do not produce
294 actinorhodin or undecylprodigiosine (Rodríguez et al. 2001). FabH is a β -oxoacyl-CoA synthase III,
295 responsible for the initiation of fatty acid biosynthesis in *S. coelicolor* and *Streptomyces glaucescens*
296 (Revill et al. 2001; Han et al. 1998). *fabH* is part of the operon for fatty acid biosynthesis *fabD-fabH-*
297 *acpP-fabF*, that shares a very similar transcriptional profile with *accBE*, indicating a common regulation
298 for both operons (Fig S3.11). Transcription of *fabG3*, which is involved in fatty acid biosynthesis in *S.*
299 *coelicolor* (SCO1346), was downregulated after glucose and glycerol additions. *S. tsukubaensis* contains
300 three *fabG* paralog genes (as well as the model species) that showed very different profiles (Fig S3.12),
301 indicating different transcriptional regulations.

302 *Effects on nitrogen assimilation*

303 Glucose addition stimulated immediately ($t_{70,7h}$) the transcription of *gltB* and *gltD*, which encode the
304 subunits of the L-glutamate synthase, while glycerol produced a steady increase (Fig S3.13). This result is
305 consistent with those observed in *S. coelicolor* and *B. subtilis*, where transcriptions of *gltBD* and *gltAB*
306 are induced by glucose (Gubbens et al. 2012; Blencke et al. 2003). The *gdhD* gene encodes a NAD-
307 glutamate dehydrogenase that is glucose-repressed and it is likely involved in glutamate utilization as
308 energy source (Gubbens et al. 2012). In accordance, the transcription of *gdhD* was downregulated
309 immediately after glucose addition (Fig S3.13). These results suggest that glucose represses glutamate
310 consumption and stimulates its biosynthesis. In agreement with these results, glucose and glycerol
311 downregulated transcription of the glutamate ABC transporter coding genes *gluABCD* (Fig S3.13).
312 Interestingly, this result is in contrast with that observed in *S. coelicolor*, in which glucose stimulates
313 transcription of the glutamate transporter (Romero-Rodríguez et al. 2016a).

314 Glutamate synthase participates in the NH_4^+ assimilation pathway along with glutamine synthetases. In
315 *S. coelicolor*, *glnA* and *glnII* encode functional glutamine synthetases (Rexer et al. 2006). In
316 *S. tsukubaensis* the orthologue genes showed a transcriptional upregulation after glucose addition (Fig
317 S3.14), although they were not filtered with the approaches used. The same transcriptional pattern was

318 detected for *amtB*, encoding an ammonium transporter (Fig S3.14). Thus, glucose might stimulate the
1 319 incorporation of NH_4^+ from the culture broth, which, in turn, might be previously secreted as a byproduct
2
3 320 of glutamate consumption.
4

5 321 Transcription of *glnR*, encoding the main nitrogen transcriptional regulator in *Streptomyces* (Fink et al.
6 322 2002), was permanently upregulated after glucose addition, whilst glycerol produced only a transient
7
8 323 activation. On the contrary, transcription of *glnRII*, a second nitrogen transcriptional regulator, was
9
10 324 mainly stimulated after glycerol addition (Fig S3.14).
11

12 325 *Effects on sulfate and phosphate assimilation*

13

14 326 The three carbon sources, but mainly glycerol, activated the sulfate reduction assimilatory pathway. The
15 327 *cysHCDN* operon, involved in the transformation of sulfate to sulfite, increased its mRNA levels at $t_{70.7\text{h}}$
16 328 (glycerol addition) or $t_{72\text{h}}$ (glucose addition). A similar pattern was shown for the adjacent genes *sirA*,
17
18 329 which product catalyses the reduction of sulfite to sulfide (Fischer et al. 2012), and the STSU_06028-
20 330 STSU_06043 operon, which encodes a Nit/Tau family transport system (Fig S3.15). Nit/Tau family
21 331 transporters are related to the incorporation of nitrates, bicarbonate, taurine or aliphatic sulfonates. Genes
22 332 for a second Nit/Tau family transporter (STSU_03564-03574), a hypothetical protein (STSU_03554), a
23 333 sulfatase (STSU_03559) and a Crp family transcriptional regulator (STSU_03579) showed the same
24
25 334 profiles (Fig S3.16). Both transporters (STSU_06028-STSU_06043 and STSU_03564-03574) show
26
27 335 homology to the *tauABCD* system of *E. coli*, which is involved in the incorporation of sulfonates under
28
29 336 sulfur starvation (van der Ploeg et al. 2001). The transcriptional profiles of the second transporter
30 337 (STSU_03564-03574) indicate a carbon source dependent induction, whilst genes encoding the first
31 338 transporter already showed high transcription values before carbon source addition. The effect of carbon
32
33 339 sources on the transcription of these genes might reflect a stimulation of sulfur assimilation by a rich
34
35 340 nutritional status.
36
37

38 341 In a similar manner, the carbon sources stimulated phosphate transport, since all the additions increased
39 342 transcription of the phosphate transporter encoded by the *pstSCAB* operon (Fig S3.17). The *phoRP* operon
40 343 (encoding the two-component system that governs the *pho* regulon; Wanner 1993) and the divergent
41 344 *phoU*, showed a similar transcriptional pattern, although their transcriptional activation was significant
42
43 345 only after glucose and glycerol additions (Fig S3.17). Finally, transcription of STSU_16912, which is
44
45 346 likely to encode a phosphatase and belongs to the *S. coelicolor pho* regulon (SCO3790; Sola-Landa et al.
46
47 347 2008) showed an equivalent transcriptional pattern, although the increase was significant only after
48
49 348 glucose addition (Fig S3.17). The transcriptional induction of phosphate transporters and scavengers
50 349 suggests an increased need of phosphate for the transport and metabolism of the carbon sources.
51
52 350 Moreover, this is a new evidence of the cross-regulation between carbon and phosphate metabolism,
53 351 which has been documented before. For example, in *S. lividans* PstS is accumulated in the media in the
54 352 presence of certain carbon sources (Díaz et al. 2005); in *S. coelicolor* transcriptions of *glpQ1* and *glpQ2*
55 353 (encoding glycerophosphodiester phosphodiesterases) are regulated not only by phosphate concentration
56
57 354 but also by the carbon sources present in the medium (Santos-Beneit et al. 2009).
58
59

60 355 *Effects on amino acid metabolism*

61
62
63
64
65

356 Carbon source additions affected the transcription of amino acid metabolism genes differently, some of
357 these changes were limited to a transient activation and some were more drastic and permanent. Glucose
358 activated the transcription of genes involved in aspartate catabolism (i.e. the *ask-asd* operon, Fig S3.18),
359 histidine synthesis (i.e. *hisCBHAF*; *hisD* and *hisI* genes lack valid probes in the microarrays; Fig S3.19).
360 Although not filtered with our approaches, we observed that tryptophan biosynthetic genes were slightly
361 upregulated by glucose and glycerol (i.e. *trpE*, *trpC* and *trpBA*; Fig S3.20).

362 The biosynthetic pathway of serine, glycine, threonine and methionine is depicted in Fig 3. Glucose
363 increased at $t_{70.7h}$ the mRNA levels of the D-3-phosphoglycerate dehydrogenase coding gene *serA* (serine
364 biosynthesis), the L-threonine 3-dehydrogenase coding gene *tdh*, and the 2-amino-3-ketobutyrate
365 coenzyme A ligase coding gene *kbl* (involved in threonine-glycine interconversion; see Fig S3.21). The
366 first step of serine biosynthesis, catalyzed by the *serA*, is also the gate to the biosynthesis of threonine and
367 glycine (see Fig 3). In addition, serine is the precursor of the sulfur-containing amino acids cysteine and
368 methionine (Fig 3).

369 All the carbon sources upregulated the transcription of cysteine and methionine metabolic genes. The
370 transcription values of *cysM* (encoding a cysteine synthase that converts acetyl-L-serine and sulfide into
371 cysteine) indicate a constitutive high transcription that is activated at $t_{70.7h}$ and t_{72h} after glycerol and
372 glucose additions, respectively (Fig S3.22). It is worthy to mention that in the *S. tsukubaensis* genome, we
373 found two *cysM* orthologues, STSU_31680 and STSU_15012, and the last one showed an *fkf*-like
374 transcriptional profile (Fig S3.22).

375 Glucose and glycerol additions increased the transcription of two putative cysteine dioxygenase coding
376 genes (STSU_22610 and STSU_08058; Fig S3.23). Although distantly located, the close similarity of
377 their profiles through all the time series (not shown), indicated a coordinated regulation. Cysteine
378 dioxygenases convert cysteine to L-cysteine sulfinic acid, which, in mammals is used for the generation of
379 pyruvate and sulfate (by aspartate aminotransferase activity) or hypotaurine (by cysteine sulfinic acid
380 decarboxylase activity). In bacteria no cysteine sulfinic acid decarboxylase activity has been reported and,
381 thus, it seems unlikely that cysteine sulfinic acid acts as precursor for taurine formation (Dominy et al. 2006).

382 The *S. tsukubaensis* genome contains two aspartate aminotransferase coding genes (*aspC* and
383 STSU_27731). Both of them showed a transcriptional activation at $t_{70.7h}$ after glycerol addition although
384 they were not filtered (Fig S3.24). Thus, glycerol addition might enhance the flux from cysteine to
385 pyruvate and sulfate. Glycerol addition stimulated the formation of L-methionine from L-homoserine and
386 Acetyl-CoA (see Fig 3) through the transcriptional upregulation of *metH* (encoding a 5-
387 methyltetrahydrofolate-homocysteine S-methyltransferase) and STSU_01830-STSU_01835, which is
388 likely to encode the *metBX* operon (Fig S3.25).

389 *Glucose and glycerol additions increase transcription of stress response genes*

390 Both glycerol and glucose additions stimulated transcription of several genes involved in oxidative stress
391 response at $t_{70.7h}$ and t_{72h} , respectively (*ahpC*, *ahpD* and *oxyR*; Fig S3.26a). Genes *ahpC*, *ahpD* encode
392 alkyl hydroperoxide reductases and are directly activated by the transcriptional regulator OxyR (Hahn et

393 al. 2002). These three genes maintained significantly higher mRNA levels during the FK506 producing
394 phase after glucose and glycerol additions than in the control condition. In fact, mRNA levels decreased
395 after 89 h in the maltose added cultures (Fig S3.26b). Glycerol addition increased specifically the
396 transcription of several genes involved in disulphide stress response at $t_{70.7\text{ h}}$ such as the regulatory operon
397 *sigR-rsrA* and the thiorredoxin and thiorredoxin reductase coding genes *trxA* and *trxB*. The thiorredoxin
398 coding gene *trxC* was also upregulated at $t_{70.7\text{ h}}$ after glucose addition (Fig S3.26). Nevertheless, these
399 changes were transient and the mRNA levels of these genes during the FK506 production phase were
400 similar in the three experimental conditions (data not shown).

401 The main source of oxidative stress in the cultures might be the activity of the respiratory chain. For
402 example, in *E. coli* as much as 87 % of the H_2O_2 is generated by this mean (González-Flecha and Demple
403 1995). Thus, the activation of genes involved in oxidative and disulphide stress might reflect an increased
404 flux through the respiratory chain. Any of the three additions increased the mRNA levels of the NAD^+
405 synthase coding gene *nadE*, which might indicate a situation of low NAD^+ availability. We also observed
406 a downregulation in the transcription of the *nuo* operon, encoding the NADH dehydrogenase I, which is
407 responsible for the regeneration of NAD^+ in the respiratory chain. The repression was stronger in the case
408 of glycerol addition (Fig S3.27). Considering that in *E. coli*, the *nuo* operon is repressed in anaerobic
409 conditions, but also under high glycolytic fluxes (Vemuri et al. 2006), these results are in agreement with
410 the increased respiratory activity suggested above.

411 *Nucleotide metabolism, transcription and translation*

412 Glucose activated rapidly transcription of genes for *de novo* biosynthesis of pyrimidines from
413 L-glutamine to UMP (*pyrR*, *pyrBC*-STSU_29616-*pyrAa-pyrA-pyrD*, *pyrF*; Fig S3.28). Genes for the
414 biosynthesis of purines (operon *purNH*) were transiently repressed by glucose and glycerol at $t_{70.7\text{ h}}$, and
415 activated at $t_{72\text{ h}}$ by glucose (Fig S3.29). Meanwhile *deoD* (STSU_12420), which product is involved in
416 the nucleotide salvage pathway, showed just the opposite profile (Fig S3.29). Besides, transcription of
417 adenylate kinase gene *adk* was permanently upregulated after glucose addition (Fig S3.30). The encoded
418 enzyme contributes to the homeostasis of adenine nucleotides catalyzing the reversible reaction
419 $\text{ADP} + \text{ADP} \leftrightarrow \text{ATP} + \text{AMP}$.

420 The effect of glucose was extended to genes related with transcription and translation processes. It
421 stimulated transcription of *rpoA* and *rpoC* at $t_{72\text{ h}}$, encoding subunits of the RNA polymerase (Fig S3.31;
422 *rpoA* was not filtered in the analysis but showed the same transcriptional profile than *rpoC*) and up to 35
423 genes encoding ribosomal proteins (Fig S3.32 and Fig S3.33; note that not all these genes were filtered in
424 the analysis but they share the same profile). In addition, we detected several genes activated by glucose
425 that did not pass the filters used in the analysis such as the translation initiation factor gene *infA* (Fig
426 S3.34), the pseudouridine tRNA synthase *truA* and the phenylalanine tRNA ligase *pheST* operon (Fig
427 S3.34). All the additions activated the transcription of *prfB*, encoding the peptide chain release factor 2
428 (Fig S3.34).

429 Glucose promoted mRNA turnover to adapt the transcriptome to a new metabolic background. For
430 example, the mRNA levels of *rns* (which encodes the ribonuclease E, a protein likely to be part of a RNA
431 degradosome-like complex in *S. coelicolor*; Lee et al. 2003) increased after the addition (Fig S3.35). It
432 also stimulated transcription of STSU_18582, encoding an ATP-dependent RNA helicase (Fig S3.35).

433 Several heat shock proteins (Hsps) that serve as molecular chaperones or proteases were induced after the
434 additions. Hsps are not only involved in the stress response, they also play crucial roles under normal
435 conditions by assisting in the folding of new polypeptides (Hartl 1996). Thus, the additions might
436 stimulate the formation of new polypeptides. Transcription of the chaperone coding gene *groEL*, which is
437 induced under acidic and heat stress (Kim et al. 2008; de León et al. 1997), was significantly
438 downregulated after all the additions (at $t_{70.7\text{h}}$ for glucose addition and at $t_{72\text{h}}$ for glycerol and maltose
439 additions). The mRNA levels of *hspR*, encoding the heat-shock regulatory system regulator, increased
440 after all the additions and, as expected, the transcriptional profile of the target operon *dnaK-grpE-dnaJ*-
441 was very similar (Fig S3.36; Bucca et al. 2009). In addition, the protease coding gene *lon*, which is a
442 direct target of HspR (Bucca et al. 2003) increased its transcription after all the additions (Fig S3.36).

443 Interestingly, two hours after glucose addition transcription of *pcrA* was specifically downregulated. This
444 gene encodes the proteasome subunit alpha. We also found a set of genes related to the proteasome
445 complex (*pcrB*-STSU_28817-STSU_28822-*arcAA*) that were specifically downregulated by glucose,
446 although they were not filtered with our approach (Fig S3.37). It must be noted that a link between
447 proteasome and stress-responsive proteins has been suggested before since mutant strains show an
448 increased resistance to certain hydroperoxides (De Mot et al. 2007). Thus, transcriptional downregulation
449 of the proteasome coding genes might give an advantage under the oxidative stress situation generated by
450 the additions.

451 **Transcriptomics during the stationary growth phase: effects of the carbon sources on antibiotic** 452 **production and morphological differentiation**

453 *Transcriptional patterns of the fkb cluster genes*

454 The transcriptomic profiles of the *fkb* cluster under the control condition allowed us to identify different
455 transcriptional patterns (see Fig 4) which correlate well with the transcriptional units proposed by
456 Ordoñez-Robles and coworkers (2016). Transcription of *fkbR* (encoding a LysR transcriptional regulator)
457 and the *all* subcluster genes *allMNPOS* was low throughout the temporal series, in accordance with that
458 reported before (Ordóñez-Robles et al. 2016). The operon *tcs6-fkbQ-fkbN*, which is transcribed in a single
459 mRNA from two independent promoters (one *fkbN*-dependent and other *fkbN*-independent; Ordóñez-
460 Robles et al. 2016), increased its transcription preceding FK506 production in a two-phase fashion: first
461 from 80 h to 89 h (corresponding to phosphate depletion), and later from 92 h to 100 h. The rest of genes,
462 encoding most of the structural genes, showed a transcriptional activation following the increase in *fkbN*
463 mRNA levels (i.e. from 92 h), which is in agreement with their FkbN dependency (Ordóñez-Robles et al.
464 2016). In view of these results we can conclude that glucose and glycerol exert their effect on FK506
465 production at least at the transcriptional level. Considering that *fkbN* transcription is not strongly

1 466 autoregulated (Ordóñez-Robles et al. 2016), a key transcriptional regulator or sigma factor might be
2 467 absent under our repressing experimental conditions.

3
4 468 *Effects on genes related to morphological and biochemical differentiation*

5
6 469 The addition of the carbon sources downregulated permanently the transcription of genes involved in
7 470 biochemical and physiological differentiation. Transcription of the RNA polymerase sigma factor coding
8 471 genes *hrdA* and *bldN* was downregulated at $t_{70.7h}$ after glucose and glycerol additions (Fig S3.38a) and the
9 472 decrease in their transcription levels was maintained throughout the cultures (Fig S3.38b). Transcription
10 473 of *hrdA* correlates with the formation of aerial mycelia in *Streptomyces aureofaciens* (Kormanec and
11 474 Farkasovský 1993) and might control secondary metabolism genes (Strakova et al. 2014). BldN is part of
12 475 the signaling cascade that leads to morphological differentiation in the genus *Streptomyces* and its
13 476 repression by glucose has been reported previously (Gubbens et al. 2012; Romero-Rodríguez et al.
14 477 2016a).

15
16
17 478 The BldK transporter is considered to be involved in the detection of the signal leading to morphological
18 479 differentiation in this genus (Nodwell et al. 1996). Transcription of the *bldK* operon was downregulated at
19 480 t_{72h} after glucose and glycerol additions (Fig S3.39a) and this response was maintained through the
20 481 culture (Fig S3.39b). A second oligopeptide transporter operon (STSU_09304-STSU_09324) was
21 482 negatively regulated at $t_{70.7h}$ after glucose addition (Fig S3.40a and b). This transporter has been shown to
22 483 be related with morphological differentiation in *S. coelicolor* and repressed by glucose (Park et al. 2005;
23 484 Romero-Rodríguez et al. 2016b).

24
25 485 Glucose addition affected specifically transcription of *wblA*, encoding a key factor for sporulation in
26 486 several *Streptomyces* species (Rabyk et al. 2011; Kang et al. 2007; Fowler-Goldsworthy et al. 2011). We
27 487 also detected an increase in transcription of *obg* after glucose and glycerol additions (Fig S3.41a and b).
28 488 This gene encodes a membrane-bound GTPase which avoids aerial mycelium formation in *S. coelicolor*
29 489 (Okamoto and Ochi 1998). Obg proteins act as sensor of the energetic status of the cell and serve as
30 490 connectors among different pathways (reviewed by Kint et al. 2014).

31
32
33 491 Crp is a key player of *E. coli* CCR and a master regulator of antibiotic production in *S. coelicolor*
34 492 although it seems to be not involved in *Streptomyces* CCR (Gao et al. 2012). Thus, given its relevance,
35 493 we search for *S. tsukubaensis* genes encoding regulators from the Crp family and identified three genes:
36 494 *crp*, *eshA* and STSU_03579 (Fig S3.42a and b). *crp* showed a constitutive transcription whilst
37 495 transcription of STSU_03579 was transiently upregulated by glycerol. Glucose and glycerol additions
38 496 decreased the mRNA levels of *eshA*, which product regulates antibiotic production in *S. coelicolor* and
39 497 *Streptomyces griseus* (Kawamoto et al. 2001; Saito et al. 2006). The two genes located immediately after
40 498 *eshA* (STSU_03589 and STSU_03594) showed the same transcriptional pattern (Fig S3.42). In
41 499 *S. coelicolor*, their ortholog genes are involved in the biosynthesis of the volatile metabolite methyl-
42 500 isoborneol (Wang and Cane 2008).

43
44
45
46
47
48
49
50
51
52 501 *fkbN-like transcriptional profiles*

502 Genes showing transcriptional profiles similar to that of *fkbN* might be involved in FK506 production or
1 503 precursor supply and thus, they might be useful candidates for genetic engineering of the strains to
2 strength production of this macrolide. In order to find such candidates, we searched for genes showing a
3 504 transcriptional profile with a Pearson correlation coefficient equal or higher than 0.9 respect to the
4 505 transcriptional profile of *fkbN*. By this means we identified 80 genes that are summarized in Table S4.
5 506

6 507 Among the genes predicted to encode proteins with a regulatory role related to morphological
7 508 differentiation, we identified *ramR* (Fig S3.43), whose product controls the expression of the *ram* operon,
8 509 involved in the transition from vegetative to aerial growth in *S. lividans* (Keijser et al. 2002).
9 510 Transcription of *atrA* showed also an *fkbN*-like profile (see Fig S3.43). AtrA is a TetR transcriptional
10 511 regulator that activates transcription of the pathway specific regulators *actII-orf4* and *strR* in *S. coelicolor*
11 512 and *S. griseus*, respectively (Uguru et al. 2005; Vujaklija et al. 1993). It also regulates in a positive
12 513 manner the daptomycin cluster of *Streptomyces roseosporus* (Mao et al. 2015).

13 514 As a second approach, we focused our attention in the transcriptional profiles of the orthologues of well
14 515 known *S.coelicolor* secondary metabolism regulators (reviewed by van Wezel and McDowall 2011). The
15 516 transcriptional patterns of those showing a positive correlation with the transcription of the *fkb* cluster
16 517 (see Table S5) are depicted in Fig S3.44 and S3.45. Among them, *afsR* is an interesting candidate for
17 518 further studies since it has been found to be overexpressed in a *S. tsukubaensis* FK506-overproducing
18 519 strain (Du et al. 2014).

19 520 Among the genes encoding biosynthetic functions related to the secondary metabolism and showing *fkbN*-
20 521 like profiles we identified STSU_07618 and *ppt1* (Fig S3.46). These genes encode a type II thioesterase
21 522 and a 4'-phosphopantetheynil transferase which transcription has been reported to be affected by FkbN
22 523 inactivation (Ordóñez-Robles et al. 2016). In addition, the product of the *ppt1* orthologue is involved in
23 524 FK506 production in *S. tsukubaensis* L19 (Wang et al. 2016). We also identified a *whiE* gene which is
24 525 related to the production of the spore pigment (Davis and Chater 1990).

25 526 **DISCUSSION**

26 527 In this work we report for the first time that glucose and glycerol block FK506 production in
27 528 *S. tsukubaensis*. The lack of transcriptional activation of the *fkb* cluster indicates that both sugars exert
28 529 their role at least at the transcriptional level. To our knowledge, this is the first report on the repressing
29 530 role of glucose in *S. tsukubaensis*, since Yoon and Choi (1997) reported no differences in FK506
30 531 production in liquid cultures containing glucose 0.17 M (3 % w/v) and Martínez-Castro and coworkers
31 532 (2013) did not detect carbon repression of FK506 biosynthesis on ISP4 liquid media in the presence of
32 533 glucose 0.22 M (2 % w/v). Nevertheless, the differences in media composition and the presence of
33 534 glucose from the beginning of the cultures might account for such different results.

34 535 This work represents the first genome-wide study on the effects of glycerol as a repressing carbon source
35 536 in *Streptomyces*. Using a second repressing carbon source enables us to distinguish between general and
36 537 specific regulatory mechanisms. In fact, we identified common transcriptional patterns but also different
37 538 responses between glucose and glycerol experimental conditions and we can conclude that the effect of

539 glycerol on central carbon pathways is much narrower than that of glucose. Both sources stimulated
1 540 transcription of genes involved in DNA replication and transcription and, as expected from the concept of
2
3 541 CCR, downregulated genes encoding alternative carbon source transporters. Several genes related to
4 542 sulfate and phosphate assimilation increased their mRNA levels in response to the additions, highlighting
5
6 543 the importance of cross-regulation between nutritional networks. Glucose and glycerol decreased
7 544 transcription of key genes involved morphological and biochemical differentiation throughout the
8
9 545 cultures. As it has been suggested before for glucose (Romero-Rodríguez et al. 2016b), preferred carbon
10 546 sources might block the signaling cascade leading to differentiation at very early stages such as the
11 547 transport of certain oligopeptides. As in the model species, we identified a permanent transcriptional
12 548 repression of the genes encoding the oligopeptide transporters *bldK* and STSU_09304-STSU_09324
13 549 (orthologue to SCO5480-SCO5476). Interestingly, although both operons share a similar transcriptional
14 550 pattern along the cultures, the response to carbon addition of STSU_09304-STSU_09324 was fastest than
15 551 that of *bldK*. The predicted products of the lipoprotein coding genes of both transporters show a 27.8 % of
16 552 identity and a 43.8 % of similarity. Thus, we consider this transporter as a new promising candidate for
17
18 553 the study of differentiation in *Streptomyces*. Nevertheless, the lack of transcription of key developmental
19 554 and *fbk* genes is likely to be related with the absence of certain transcriptional regulators or sigma factors
20
21 555 such as *hrdA* or *bldN*.

26 556 In the case of glucose several omic studies are available to compare our results. We obtained
27 557 experimental evidence supporting the different transcriptional regulation of paralog genes encoding the
28 558 same enzymatic activity such as the *pfkA*, *gdh* and *fabG* genes. It is worthy to mention the differences
29 559 detected between *S. tsukubaensis* and the model species *S. coelicolor*. For example, glucose increases
30 560 transcription of the glutamate transporter operon *gltABCD* in *S. coelicolor*, since glutamate is preferred
31 561 over glucose in this species (Romero-Rodríguez et al. 2016a; van Wezel et al. 2005). In *S. tsukubaensis*
32 562 we observed the opposite response, indicating that glucose slows down glutamate consumption and might
33 563 act as preferred carbon source over glutamate. Similarly, the transcriptional behavior of the xylose
34 564 transporter genes is opposed in both species (Gubbens et al. 2012; Romero-Rodríguez et al. 2016a). In
35 565 addition, contrary to the situation in the model species, there is a lack of glucose-dependent
36 566 transcriptional activation of the glucose permease coding gene *glcP* in *S. tsukubaensis*. This raises the
37 567 question of how is glucose internalized in this species. These examples reflect the differences between
38 568 regulatory networks in *Streptomyces* species and strengthen the utilization of new models to unravel
39 569 *Streptomyces* biology.

48 570 This work also highlights the importance of performing time series designs instead of one point designs
49 571 when analyzing omic data. For example, Romero-Rodríguez and coworkers (2016b) did not detect
50 572 differences in the expression of the important transcriptional regulator AtrA (SCO4118) between
51 573 repressing and non-repressing conditions in the unique sample collected during the exponential growth
52 574 phase. In our work, we did not detect differences between experimental conditions during the exponential
53 575 growth phase, but the mRNA levels of the orthologous *atrA* gene (STSU_07858) were 3.2 times higher in
54 576 the control than in repressing conditions during the stationary phase (i.e. 100 h). Therefore, relevant
55 577 information might be lost in one point designs.

578 Finally, the identification of transcriptional regulators showing *fkbN*-like transcriptional profiles that are
1 579 involved in antibiotic production in other *Streptomyces* species (i.e. *atrA* or *afsR*) provide candidates for
2
3 580 FK506 yield improvement but also for the awakening of secondary metabolite cryptic clusters.
4

5 581 **Conflict of interest**

6 582 The authors declare no financial or commercial conflict of interest
7
8

9 583
10

11 584
12

13 585
14

15 586
16

17 587
18

19 588
20

21 589
22

23 590
24

25 591
26

27 592
28

29 593
30

31 594
32

33 595
34

35 596
36

37 597
38

39 598
40

41 599
42

43 600
44

45 601
46

47 602
48

49 603
50

51 604
52

53
54

55
56

57
58

59
60

61
62
63
64
65

605 **REFERENCES:**

- 1
2 606 Angell S, Schwarz E, Bibb MJ (1992) The glucose kinase gene of *Streptomyces coelicolor* A3(2): its
3
4 607 nucleotide sequence, transcriptional analysis and role in glucose repression. *Mol Microbiol* 6(19): 2833-
5
6 608 2844
7
8 609 Barreiro C, Martínez-Castro M (2014) Trends in the biosynthesis and production of the
9
10 610 immunosuppressant tacrolimus (FK506). *Appl Microbiol Biotechnol* 98(2): 497-507
11
12 611 Benjamini Y, Hochberg Y (1995) Controlling the False Discovery Rate: A Practical and Powerful
13
14 612 Approach to Multiple Testing. *Journal of the Royal Statistical Society, Series B (Methodological)*, 57(1):
15
16 613 289-300
17
18 614 Blencke HM, Homuth G, Ludwig H, Mäder U, Hecker M, Stülke J (2003) Transcriptional profiling of
19
20 615 gene expression in response to glucose in *Bacillus subtilis*: regulation of the central metabolic pathways.
21
22 616 *Metab Eng* 5(2): 133-149
23
24 617 Breuder T, Hemenway CS, Movva NR, Cardenas ME, Heitman J (1994) Calcineurin is essential in
25
26 618 cyclosporin A- and FK506-sensitive yeast strains. *Proc Natl Acad Sci USA* 91(12): 5372-5376
27
28 619 Bucca G, Brassington AME, Hotchkiss G, Mersinias V, Smith CP (2003) Negative feedback regulation of
29
30 620 *dnaK*, *clpB* and *lon* expression by the DnaK chaperone machine in *Streptomyces coelicolor*, identified by
31
32 621 transcriptome and in vivo DnaK-depletion analysis. *Mol Microbiol* 50(1): 153-166
33
34 622 Bucca G, Laing E, Mersinias V, Allenby N, Hurd D, Holdstock J, Brenner V, Harrison M, Smith CP
35
36 623 (2009) Development and application of versatile high density microarrays for genome-wide analysis of
37
38 624 *Streptomyces coelicolor*: characterization of the HspR regulon. *Genome Biol* 10(1): R5
39
40 625 Chen D, Zhang Q, Zhang Q, Cen P, Xu Z, Liu W (2012) Improvement of FK506 production in
41
42 626 *Streptomyces tsukubaensis* by genetic enhancement of the supply of unusual polyketide extender units via
43
44 627 utilization of two distinct site-specific recombination systems. *Appl Environ Microbiol* 78(15): 5093-
45
46 628 5103
47
48 629 Conesa A, Nueda MJ, Ferrer A, Talón M (2006) maSigPro: a method to identify significantly differential
49
50 630 expression profiles in time-course microarray experiments. *Bioinformatics* 22(9): 1096-1102
51
52 631 Davis NK, Chater KF (1990) Spore colour in *Streptomyces coelicolor* A3(2) involves the
53
54 632 developmentally regulated synthesis of a compound biosynthetically related to polyketide antibiotics. *Mol*
55
56 633 *Microbiol* 4(10): 1679-1691
57
58 634 De León P, Marco S, Isiegas C, Marina A, Carrascosa JL, Mellado RP (1997) *Streptomyces lividans*
59
60 635 *groES*, *groEL1* and *groEL2* genes. *Microbiology* 143 (Pt 11): 3563-3571
61
62 636 De Mot R, Schoofs G, Nagy I (2007) Proteome analysis of *Streptomyces coelicolor* mutants affected in
63
64 637 the proteasome system reveals changes in stress-responsive proteins. *Arch Microbiol* 188(3): 257-271
65
66 638 Díaz M, Esteban A, Fernández-Abalos JM, Santamaría RI (2005) The high-affinity phosphate-binding
67
68 639 protein PstS is accumulated under high fructose concentrations and mutation of the corresponding gene
69
70 640 affects differentiation in *Streptomyces lividans*. *Microbiology* 151(Pt 8): 2583-2592
71
72 641 Dominy Jr JE, Simmons CR, Karplus PA, Gehring AM, Stipanuk MH (2006) Identification and
73
74 642 characterization of bacterial cysteine dioxygenases: a new route of cysteine degradation for eubacteria. *J*
75
76 643 *Bacteriol* 188(15): 5561-5569
77
78 644 Du W, Huang D, Xia M, Wen J, Huang M (2014) Improved FK506 production by the precursors and

645 product-tolerant mutant of *Streptomyces tsukubaensis* based on genome shuffling and dynamic fed-batch
1 646 strategies. J Ind Microbiol Biotechnol 41(7): 1131-1143
2
3 647 Dufour YS, Wesenberg GE, Tritt AJ, Glasner JD, Perna NT, Mitchell JC, Donohue TJ (2010) chipD: a
4 648 web tool to design oligonucleotide probes for high-density tiling arrays. Nucleic Acids Res 38(Web
5
6 649 Server issue), W321-W325
7 650 Fink D, Weissschuh N, Reuther J, Wohlleben W, Engels A (2002) Two transcriptional regulators GlnR
8
9 651 and GlnRII are involved in regulation of nitrogen metabolism in *Streptomyces coelicolor* A3(2). Mol
10 652 Microbiol 46(2): 331-347
11
12 653 Fischer M, Schmidt C, Falke D, Sawers RG (2012) Terminal reduction reactions of nitrate and sulfate
13 654 assimilation in *Streptomyces coelicolor* A3(2): identification of genes encoding nitrite and sulfite
14 655 reductases. Res Microbiol 163(5): 340-348
15
16 656 Fowler-Goldsworthy K, Gust B, Mouz S, Chandra G, Findlay KC, Chater KF (2011) The actinobacteria-
17 657 specific gene *wblA* controls major developmental transitions in *Streptomyces coelicolor* A3(2).
18 658 Microbiology 157(Pt 5): 1312-1328
19
20 659 Gao B, Gupta RS (2012) Phylogenetic framework and molecular signatures for the main clades of the
21 660 phylum Actinobacteria. Microbiol Mol Biol Rev 76(1): 66-112
22
23 661 González-Flecha B, Demple B (1995) Metabolic sources of hydrogen peroxide in aerobically growing
24 662 *Escherichia coli*. J Biol Chem 270(23): 13681-13687
25
26 663 Gubbens J, Janus M, Florea BI, Overkleeft HS, van Wezel GP (2012) Identification of glucose kinase-
27 664 dependent and -independent pathways for carbon control of primary metabolism, development and
28 665 antibiotic production in *Streptomyces coelicolor* by quantitative proteomics. Mol Microbiol 86(6):1490-
29 666 507. doi: 10.1111/mmi.12072
30
31 667 Hahn JS, Oh SY, Roe JH (2002) Role of OxyR as a peroxide-sensing positive regulator in *Streptomyces*
32 668 *coelicolor* A3(2). J Bacteriol 184(19): 5214-5222
33
34 669 Han L, Lobo S, Reynolds KA (1998) Characterization of beta-ketoacyl-acyl carrier protein synthase III
35 670 from *Streptomyces glaucescens* and its role in initiation of fatty acid biosynthesis. J Bacteriol 180(17):
36 671 4481-4486
37
38 672 Hartl FU (1996) Molecular chaperones in cellular protein folding. Nature 381(6583): 571-579
39
40 673 Hopwood DA (2007) *Streptomyces* in Nature and Medicine: The Antibiotic Makers. Oxford University
41 674 Press, New York, USA
42
43 675 Hurtubise Y, Shareck F, Kluepfel D, Morosoli R (1995) A cellulase/xylanase-negative mutant of
44 676 *Streptomyces lividans* 1326 defective in cellobiose and xylobiose uptake is mutated in a gene encoding a
45 677 protein homologous to ATP-binding proteins. Mol Microbiol 17(2): 367-377
46
47 678 Kang SH, Huang J, Lee HN, Hur YA, Cohen SN, Kim ES (2007) Interspecies DNA microarray analysis
48 679 identifies WblA as a pleiotropic down-regulator of antibiotic biosynthesis in *Streptomyces*. J Bacteriol
49 680 189(11): 4315-4319
50
51 681 Kawamoto S, Watanabe M, Saito N, Hesketh A, Vachalova K, Matsubara K, Ochi K (2001) Molecular
52 682 and functional analyses of the gene (*eshA*) encoding the 52-kilodalton protein of *Streptomyces coelicolor*
53 683 A3(2) required for antibiotic production. J Bacteriol 183(20): 6009-6016
54
55 684 Keijsers B, van Wezel GP, Canters GW, Vijgenboom E (2002) Developmental regulation of the
56
57
58
59
60
61
62
63
64
65

685 *Streptomyces lividans ram* genes: involvement of RamR in regulation of the *ramCSAB* operon. J Bacteriol
686 184(16): 4420-4429

687 Kim YJ, Moon MH, Song JY, Smith CP, Hong SK, Chang YK (2008) Acidic pH shock induces the
688 expressions of a wide range of stress-response genes. BMC Genomics 9, 604

689 Kino T, Hatanaka H, Hashimoto M, Nishiyama M, Goto T, Okuhara M, Kohsaka M, Aoki H, Imanaka H
690 (1987) FK-506, a novel immunosuppressant isolated from a *Streptomyces*. I. Fermentation, isolation, and
691 physico-chemical and biological characteristics. J Antibiot (Tokyo) 40(9): 1249-1255

692 Kino T, Hatanaka H, Miyata S, Inamura N, Nishiyama M, Yajima T, Goto T, Okuhara M, Kohsaka M,
693 Aoki H (1987) FK-506, a novel immunosuppressant isolated from a *Streptomyces*. II. Immunosuppressive
694 effect of FK-506 in vitro. J Antibiot (Tokyo) 40(9): 1256-1265

695 Kint C, Verstraeten N, Hofkens J, Fauvart M, Michiels J (2014) Bacterial Obg proteins: GTPases at the
696 nexus of protein and DNA synthesis. Crit Rev Microbiol 40(3): 207-224

697 Kormanec J, Farkasovský M (1993) Differential expression of principal sigma factor homologues of
698 *Streptomyces aureofaciens* correlates with the developmental stage. Nucleic Acids Res 21(16): 3647-
699 3652

700 Lanzetta PA, Alvarez LJ, Reinach PS, Candia OA (1979) An improved assay for nanomole amounts of
701 inorganic phosphate. Anal Biochem 100(1): 95-97

702 Lee K, Cohen SN (2003) A *Streptomyces coelicolor* functional orthologue of *Escherichia coli* RNase E
703 shows shuffling of catalytic and PNPase-binding domains. Mol Microbiol 48(2): 349-360

704 Lodder J (1970) The yeasts, a taxonomic study. North Holland Publishing Company, Amsterdam, The
705 Netherlands.

706 Lounès A, Lebrihi A, Benslimane C, Lefebvre G, Germain P (1996) Regulation of spiramycin synthesis
707 in *Streptomyces ambofaciens*: effects of glucose and inorganic phosphate. Appl Microbiol Biotechnol
708 45(1-2): 204-211

709 Magasanik B (1961) Catabolite repression. Cold Spring Harb Symp Quant Biol 26: 249-256

710 Mao XM, Luo S, Zhou RC, Wang F, Yu P, Sun N, Chen XX, Tang Y, Li YQ (2015) Transcriptional
711 regulation of the daptomycin gene cluster in *Streptomyces roseosporus* by an autoregulator, AtrA. J Biol
712 Chem 290:7992–8001. doi:10.1074/jbc.M114.608273

713 Martínez-Castro M, Salehi-Najafabadi Z, Romero F, Pérez-Sanchiz R, Fernández-Chimeno RI, Martín JF,
714 Barreiro C (2013) Taxonomy and chemically semi-defined media for the analysis of the tacrolimus
715 producer '*Streptomyces tsukubaensis*'. Appl Microbiol Biotechnol 97(5): 2139-2152

716 Mehra S, Lian W, Jayapal KP, Charaniya SP, Sherman DH, Hu WS (2006) A framework to analyze
717 multiple time series data: a case study with *Streptomyces coelicolor*. J Ind Microbiol Biotechnol 33(2):
718 159-172

719 Mitchell A, Romano GH, Groisman B, Yona A, Dekel E, Kupiec M, Dahan O, Pilpel Y (2009) Adaptive
720 prediction of environmental changes by microorganisms. Nature 460(7252): 220-224

721 Nodwell JR, McGovern K, Losick R (1996) An oligopeptide permease responsible for the import of an
722 extracellular signal governing aerial mycelium formation in *Streptomyces coelicolor*. Mol Microbiol
723 22(5): 881-893

724 Ordóñez-Robles M, Rodríguez-García A, Martín JF (2016) Target genes of the *Streptomyces*
1 725 *tsukubaensis* FkbN regulator include most of the tacrolimus biosynthesis genes, a phosphopantetheinyl
2 726 transferase and other PKS genes. *Appl Microbiol Biotechnol* 100(18): 8091-103
3
4 727 Ohné M (1975) Regulation of the dicarboxylic acid part of the citric acid cycle in *Bacillus subtilis*. *J*
5 728 *Bacteriol* 122(1): 224-234
6
7 729 Okamoto S, Ochi K (1998) An essential GTP-binding protein functions as a regulator for differentiation
8 730 in *Streptomyces coelicolor*. *Mol Microbiol* 30(1): 107-119
9
10 731 Park HS, Shin SK, Yang YY, Kwon HJ, Suh JW (2005) Accumulation of S-adenosylmethionine induced
11 732 oligopeptide transporters including BldK to regulate differentiation events in *Streptomyces coelicolor*
12 733 M145. *FEMS Microbiol Lett* 249(2): 199-206
13
14 734 Park SJ, Gunsalus RP (1995) Oxygen, iron, carbon, and superoxide control of the fumarase *fumA* and
15 735 *fumC* genes of *Escherichia coli*: role of the *arcA*, *fnr*, and *soxR* gene products. *J Bacteriol* 177(21): 6255-
16 736 6262
17
18 737 Pérez-Redondo R, Santamarta I, Bovenberg R, Martín JF, Liras P (2010) The enigmatic lack of glucose
19 738 utilization in *Streptomyces clavuligerus* is due to inefficient expression of the glucose permease gene.
20 739 *Microbiology* 156(Pt 5): 1527-1537
21
22 740 Rabyk M, Ostash B, Rebets Y, Walker S, Fedorenko V (2011) *Streptomyces ghanaensis* pleiotropic
23 741 regulatory gene *wblA(gh)* influences morphogenesis and moenomycin production. *Biotechnol Lett*
24 742 33(12): 2481-2486
25
26 743 Revill WP, Bibb MJ, Scheu AK, Kieser HJ, Hopwood DA (2001) Beta-ketoacyl acyl carrier protein
27 744 synthase III (FabH) is essential for fatty acid biosynthesis in *Streptomyces coelicolor* A3(2). *J Bacteriol*
28 745 183(11): 3526-3530
29
30 746 Rexer HU, Schäberle T, Wohlleben W, Engels A (2006) Investigation of the functional properties and
31 747 regulation of three glutamine synthetase-like genes in *Streptomyces coelicolor* A3(2). *Arch Microbiol*
32 748 186(6): 447-458
33
34 749 Rodríguez E, Banchio C, Diacovich L, Bibb MJ, Gramajo H (2001) Role of an essential acyl coenzyme A
35 750 carboxylase in the primary and secondary metabolism of *Streptomyces coelicolor* A3(2). *Appl Environ*
36 751 *Microbiol* 67(9): 4166-4176
37
38 752 Romero-Rodríguez A, Rocha D, Ruiz-Villafan B, Tierrafría V, Rodríguez-Sanoja R, Segura-González D,
39 753 Sánchez S (2016a) Transcriptomic analysis of a classical model of carbon catabolite regulation in
40 754 *Streptomyces coelicolor*. *BMC Microbiol* 16(1): 77
41
42 755 Romero-Rodríguez A, Ruiz-Villafan B, Tierrafría V, Rodríguez-Sanoja R, Sánchez S (2016b) Carbon
43 756 Catabolite Regulation of Secondary Metabolite Formation and Morphological Differentiation in
44 757 *Streptomyces coelicolor* *Appl Biochem Biotechnol* 180(6): 1152-1166
45
46 758 Ruiz B, Chávez A, Forero A, García-Huante Y, Romero A, Sánchez M, Rocha D, Sánchez B, Rodríguez-
47 759 Sanoja R, Sánchez S, Langley E (2010) Production of microbial secondary metabolites: regulation by the
48 760 carbon source. *Crit Rev Microbiol* 36(2): 146-167
49
50 761 Saito A, Shinya T, Miyamoto K, Yokoyama T, Kaku H, Minami E, Shibuya N, Tsujibo H, Nagata Y,
51 762 Ando A, Fujii T, Miyashita K (2007) The *dasABC* gene cluster, adjacent to *dasR*, encodes a novel ABC
52 763 transporter for the uptake of N,N'-diacetylchitobiose in *Streptomyces coelicolor* A3(2). *Appl Environ*

764 Microbiol 73(9): 3000-3008

1 765 Saito N, Xu J, Hosaka T, Okamoto S, Aoki H, Bibb MJ, Ochi K (2006) EshA accentuates ppGpp
2 accumulation and is conditionally required for antibiotic production in *Streptomyces coelicolor* A3(2). J
3 766 Bacteriol 188(13): 4952-4961

4 767

5 768 Salehi-Najafabadi Z, Barreiro C, Rodríguez-García A, Cruz A, López GE, Martín JF (2014) The gamma-
6 butyrolactone receptors BulR1 and BulR2 of *Streptomyces tsukubaensis*: tacrolimus (FK506) and
7 769 butyrolactone synthetases production control. Appl Microbiol Biotechnol 98(11): 4919-4936

8 770

9 771 Santos-Beneit F, Rodríguez-García A, Apel AK, Martín JF (2009) Phosphate and carbon source
10 regulation of two PhoP-dependent glycerophosphodiester phosphodiesterase genes of *Streptomyces*
11 772 *coelicolor*. Microbiology 155(Pt 6): 1800-1811

12 773

13 774 Sidders B, Withers M, Kendall SL, Bacon J, Waddell SJ, Hinds J, Golby P, Movahedzadeh F, Cox RA,
14 775 Frita R, Ten Bokum AMC, Wernisch L, Stoker NG (2007) Quantification of global transcription patterns
15 776 in prokaryotes using spotted microarrays. Genome Biol 8(12): R265

16 777

17 778 Smith CP, Chater KF (1988) Structure and regulation of controlling sequences for the *Streptomyces*
18 *coelicolor* glycerol operon. J Mol Biol 204(3): 569-580

19 779

20 780 Smyth GK (2004) Linear models and empirical bayes methods for assessing differential expression in
21 microarray experiments. Stat Appl Genet Mol Biol 3, Article3

22 781

23 782 Sola-Landa A, Rodríguez-García A, Apel AK, Martín JF (2008) Target genes and structure of the direct
24 repeats in the DNA-binding sequences of the response regulator PhoP in *Streptomyces coelicolor*.
25 783 Nucleic Acids Res 36(4): 1358-1368

26 784

27 785 Solovyev V, Salamov A (2011) Automatic Annotation of Microbial Genomes and Metagenomic
28 Sequences. In Metagenomics and its Applications in Agriculture, Biomedicine and Environmental Studies
29 (Ed. R.W. Li), Nova Science Publishers, p.61-78

30 786

31 787 Strakova E, Zikova A, Vohradsky J (2014) Inference of sigma factor controlled networks by using
32 numerical modeling applied to microarray time series data of the germinating prokaryote. Nucleic Acids
33 788 Res 42(2): 748-763

34 789

35 790 Swiatek MA, Gubbens J, Bucca G, Song E, Yang YH, Laing E, Kim BG, Smith CP, van Wezel GP
36 791 (2013) The ROK family regulator Rok7B7 pleiotropically affects xylose utilization, carbon catabolite
37 792 repression, and antibiotic production in *Streptomyces coelicolor*. J Bacteriol 195(6): 1236-1248

38 793

39 794 Uguru GC, Stephens KE, Stead JA, Towle JE, Baumberg S, McDowall KJ (2005) Transcriptional
40 activation of the pathway-specific regulator of the actinorhodin biosynthetic genes in *Streptomyces*
41 795 *coelicolor*. Mol Microbiol 58(1): 131-150

42 796

43 797 van der Ploeg JR, Eichhorn E, Leisinger T (2001) Sulfonate-sulfur metabolism and its regulation in
44 *Escherichia coli*. Arch Microbiol 176(1-2): 1-8

45 798

46 799 van Wezel GP, Mahr K, König M, Traag BA, Pimentel-Schmitt EF, Willimek A, Titgemeyer F (2005)
47 GlcP constitutes the major glucose uptake system of *Streptomyces coelicolor* A3(2). Mol Microbiol
48 800 55(2): 624-636

49 801

50 802 van Wezel GP, McDowall KJ (2011) The regulation of the secondary metabolism of *Streptomyces*: new
51 links and experimental advances. Nat Prod Rep 28(7): 1311-1333

52 803

53 804 van Wezel GP, White J, Bibb MJ, Postma PW (1997) The *malEFG* gene cluster of *Streptomyces*

804 *coelicolor* A3(2): characterization, disruption and transcriptional analysis. Mol Gen Genet 254(5): 604-
1 805 608
2
3 806 Vemuri GN, Altman E, Sangurdekar DP, Khodursky AB, Eiteman MA (2006) Overflow metabolism in
4 807 *Escherichia coli* during steady-state growth: transcriptional regulation and effect of the redox ratio. Appl
5 808 Environ Microbiol 72(5): 3653-3661
6
7 809 Vujaklija D, Horinouchi S, Beppu T (1993) Detection of an A-factor-responsive protein that binds to the
8 810 upstream activation sequence of *strR*, a regulatory gene for streptomycin biosynthesis in *Streptomyces*
9 811 *griseus*. J Bacteriol 175(9): 2652-2661
10
11 812 Wang CM, Cane DE (2008) Biochemistry and molecular genetics of the biosynthesis of the earthy
12 813 odorant methylisoborneol in *Streptomyces coelicolor*. J Am Chem Soc 130(28): 8908-8909
13
14 814 Wang YY, Zhang XS, Luo HD, Ren NN, Jiang XH, Jiang H, Li YQ (2016) Characterization of Discrete
15 815 Phosphopantetheinyl Transferases in *Streptomyces tsukubaensis* L19 Unveils a Complicate
16 816 Phosphopantetheinylation Network. Sci Rep 6: 24255
17
18 817 Wanner BL (1993) Gene regulation by phosphate in enteric bacteria. J Cell Biochem 51(1): 47-54
19
20 818 Yoon YJ, Choi CY (1997) Nutrient Effects on FK-506, a New Immunosuppressant, Production by
21 819 *Streptomyces* sp. in a Defined Medium. J Ferment Bioeng 83(6): 599-603.doi:10.1016/s0922-
22 820 338x(97)81145-2
23
24 821
25
26
27
28 822
29
30
31 823
32
33 824
34
35 825
36
37
38 826
39
40 827
41
42 828
43
44
45 829
46
47 830
48
49 831
50
51
52 832
53
54 833
55
56
57 834
58
59 835
60
61
62
63
64
65

836 **Figure legends**

1
2 837 **Fig 1. Growth, FK506 production and phosphate depletion patterns in the cultures.** A) Growth is
3
4 838 represented as the average of the dry weight values from two replicates (glucose, glycerol and maltose
5 839 supplemented conditions are represented with rhomboids, circles and squares, respectively). B) FK506
6
7 840 production in each culture broth. C) Phosphate depletion pattern in each culture. Note that phosphate is
8
9 841 depleted between 80 h and 89 h, since its concentration falls under 100 μ M in all the replicates. For
10 842 panels B and C the two replicates of glucose (rhomboids), glycerol (circles) and maltose (squares)
11 843 supplemented cultures are represented with black and grey lines.

12
13
14 844 **Fig 2. Schematic representation of central carbon pathways and the effect of glucose addition on**
15 845 **involved genes.** Genes showing transcriptional upregulation (\uparrow) or downregulation (\downarrow) are indicated.
16
17 846 Note that for the step in which several paralogs are involved, only those significantly affected are
18 847 depicted.

19
20
21 848 **Fig 3. Schematic representation of the serine, glycine, threonine and methionine biosynthetic**
22 849 **pathways and the effect of glucose addition.** Genes showing transcriptional upregulation are indicated
23
24 850 above the corresponding arrow.

25
26 851 **Fig 4. Gene organization of the *fkb* cluster (a) and transcriptional patterns detected under the three**
27 852 **experimental conditions (b).** In panel A, the transcriptional units detected by Ordóñez-Robles et al.
28
29 853 (2016) are indicated in black frames. In panel B, the average M_g values of selected genes are depicted,
30 854 except for *fkbR* and *fkbG*, which are represented independently. In the representation of average M_g
31 855 values error bars have been omitted to facilitate the visualization of the results. Maltose, glucose and
32 856 glycerol conditions are represented in black, red and blue lines, respectively.

33
34
35
36 857 **Fig S1. Validation of microarray data by RT-qPCR.** The correlation between the \log_2 fold changes
37 858 in the transcript levels of target genes obtained by microarray and RT-qPCR is represented. Comparisons
38
39 859 were performed between 89 h samples from different culture conditions (i. e. glucose vs maltose) but also
40 860 between time samples from the same experimental conditions (i. e. 89 h and 70 h from glucose cultures).

41
42
43 861 **Fig S2. Representation of the group of the genes selected for the analysis.** The statistical analysis with
44 862 limma (blue circle) yielded 203 genes significantly affected after the additions with 2-fold or greater
45 863 changes at 70.7 h. The statistical analysis using maSigPro (red circle) revealed differences in 255 genes
46 864 showing $R^2 \geq 0.9$. The functional analysis was focused on the set of 361 genes listed in Table S3.

47
48
49
50 865 **Fig S3. Transcriptional profiles of selected genes.** The \log_2 transcription values (M_g) of selected genes
51 866 along the cultures are depicted for the three experimental conditions. From left to right, the panels
52 867 correspond to the glucose, glycerol and maltose (control) conditions. For some figures, we depict a forth
53 868 panel on the right indicating the average M_g transcription values of selected genes under the three
54 869 experimental conditions to facilitate the comparison of the profiles (in this case, glucose, glycerol and
55 870 maltose additions are represented as red, blue and black lines). Error bars are omitted to facilitate the

871 visualization of the results. In figures 4.11 and 4.19, transcription of *fabD*, *hisD* and *hisI* is not
872 represented since the microarrays used lacked probes for these genes.

1
2
3
4
5
6
7
8
9
10
11
12
13
14
15
16
17
18
19
20
21
22
23
24
25
26
27
28
29
30
31
32
33
34
35
36
37
38
39
40
41
42
43
44
45
46
47
48
49
50
51
52
53
54
55
56
57
58
59
60
61
62
63
64
65

Figure 1

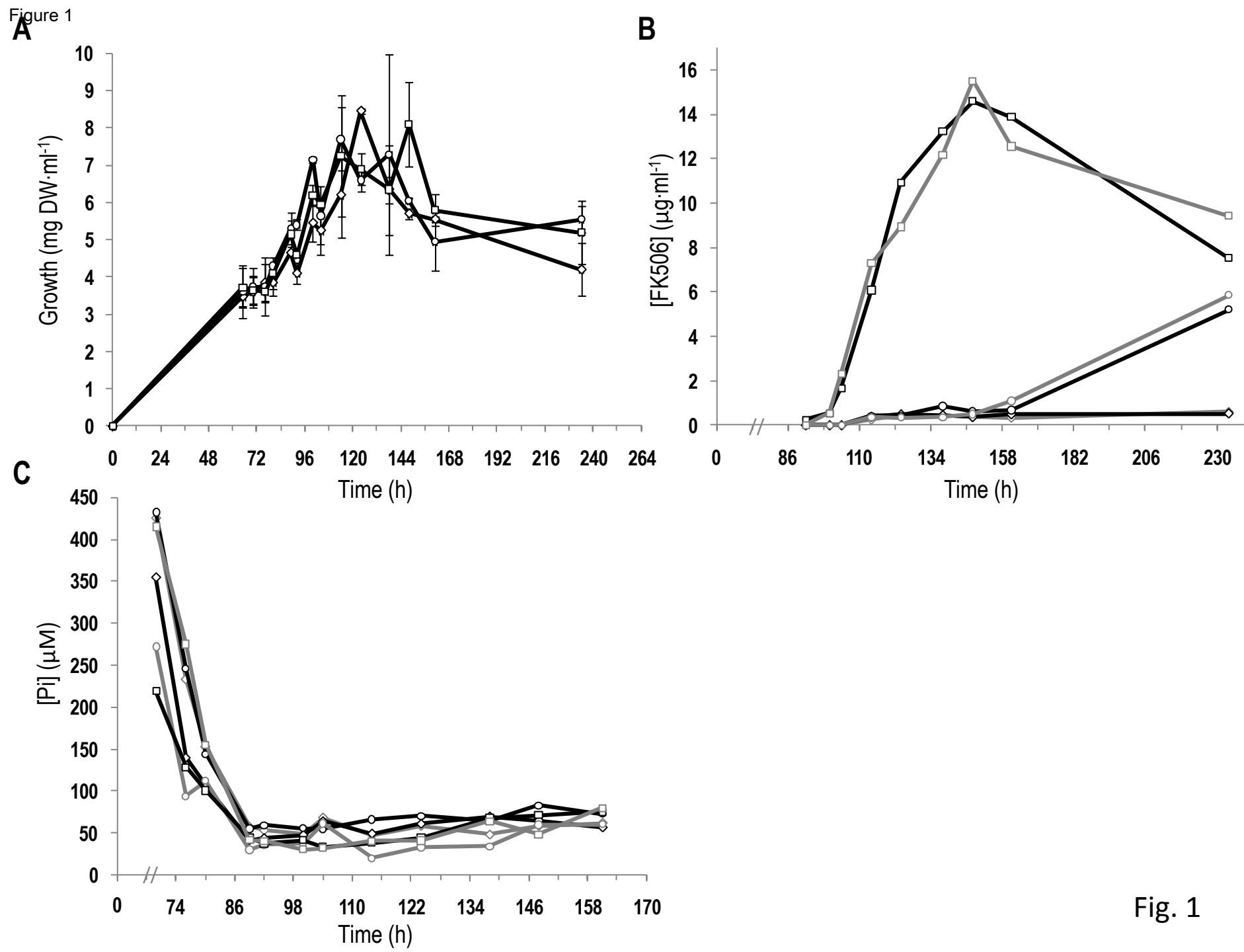


Fig. 1

Figure 2

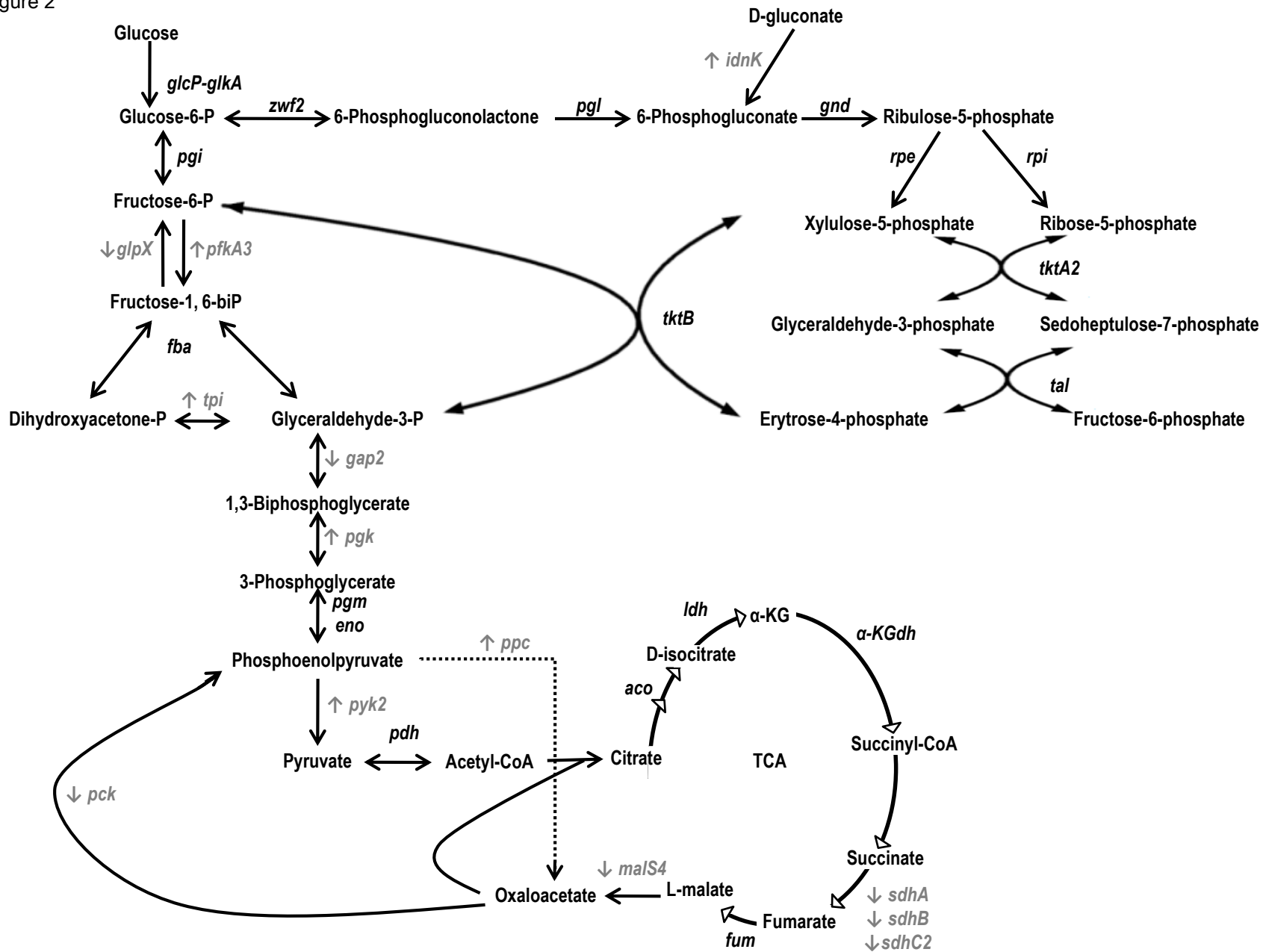


Fig. 2

Figure 3

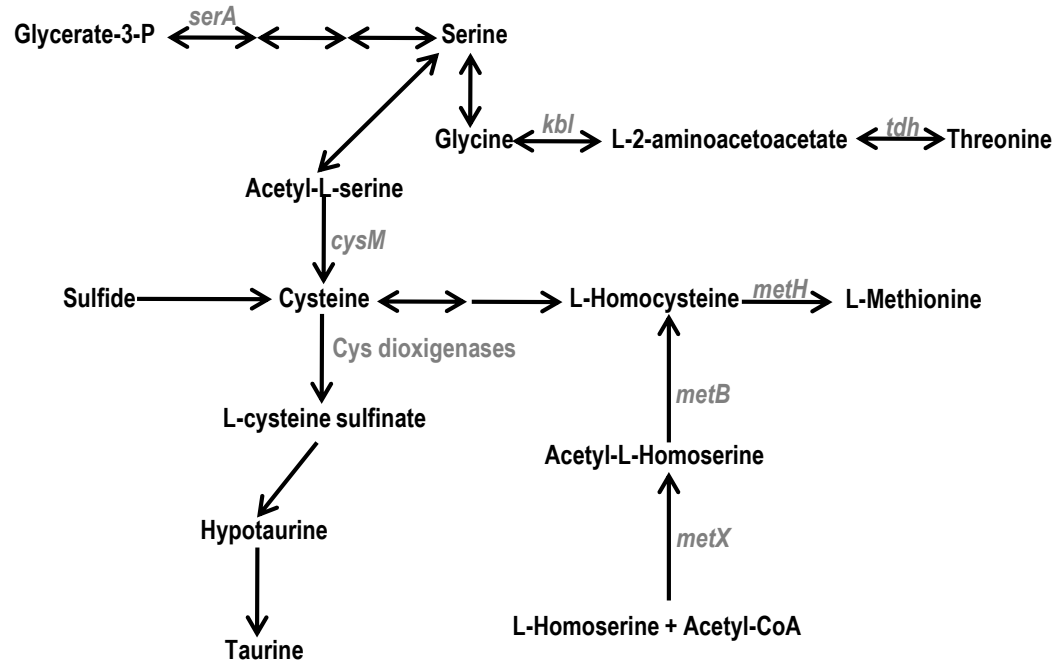


Fig. 3

Figure 4

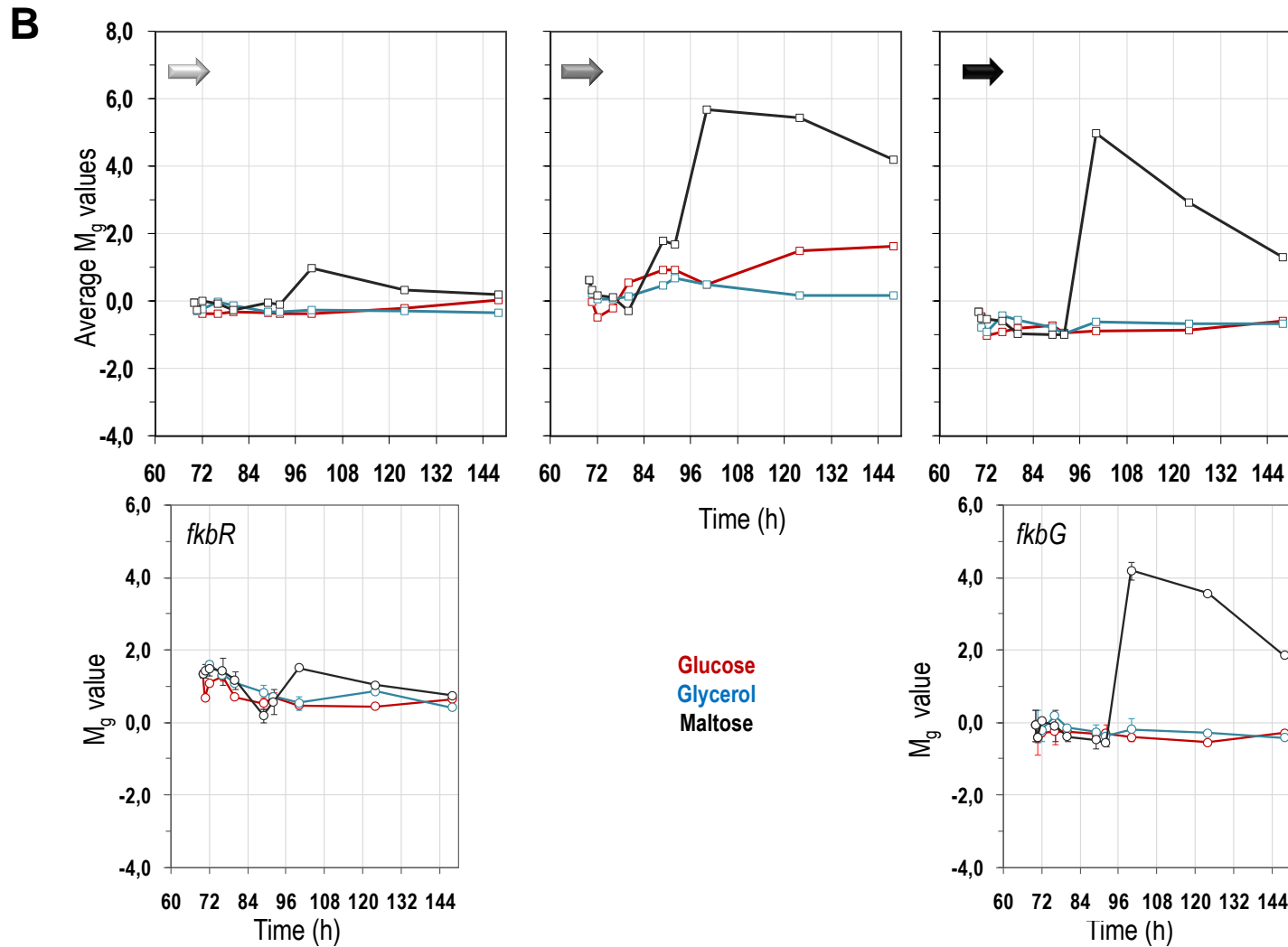
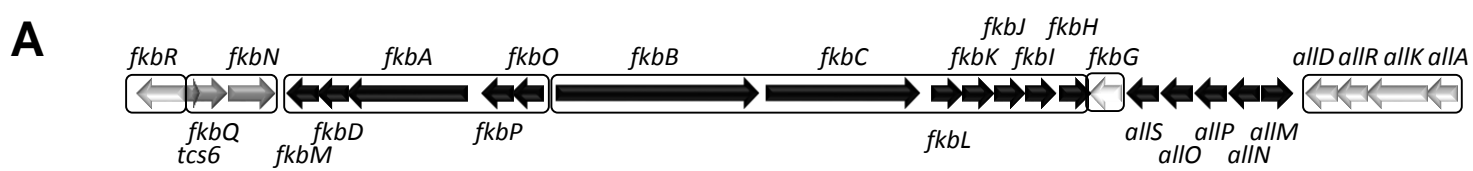
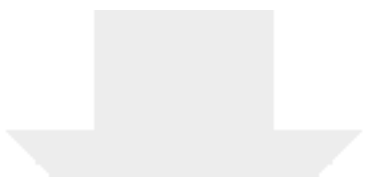

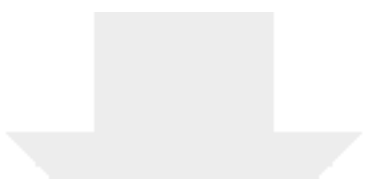


Fig. 4

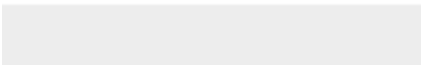



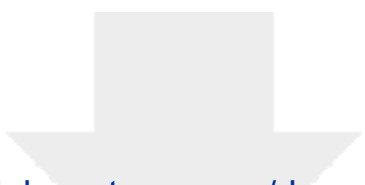
Click here to access/download
Supplementary Material
Table S1.pdf






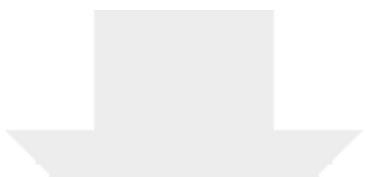
Click here to access/download
Supplementary Material
Table S2.pdf






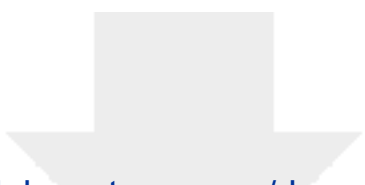
Click here to access/download
Supplementary Material
Table S3.pdf






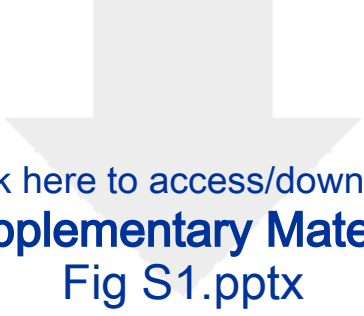
Click here to access/download
Supplementary Material
Table S4.pdf






Click here to access/download
Supplementary Material
Table S5.pdf






Click here to access/download
Supplementary Material
Fig S1.pptx



Click here to access/download
Supplementary Material
Fig S2.pptx



Click here to access/download
Supplementary Material
Fig S3.pptx